Structural Engineering and Mechanics, Vol. 40, No. 3 (2011) 411-429
DOI: http://dx.doi.org/10.12989/sem.2011.40.3.411

Behavior of reinforced concrete beams filled with demolished concrete lumps

Bo Wu*[1], Zhe Xu[1,3a], Zhongguo John Ma[2b], Qiongxiang Liu[3c] and Wei Liu[1,3a]

[1]*State Key Laboratory of Subtropical Building Science, Department of Civil Engineering, South China Univ. of Technology, Guangzhou 510640, China*
[2]*Department of Civil and Environmental Engineering, University of Tennessee Knoxville, 223 Perkins Hall, Knoxville, TN 37996-2010, USA*
[3]*Shenzhen General Institute of Architectural Design and Research, Shenzhen 518031, China*

(Received December 17, 2010, Revised May 2, 2011, Accepted August 18, 2011)

Abstract. In the past decades, recycling use of demolished concrete was almost limited to the types of recycled coarse aggregate with a size of about 5-40 mm and recycled fine aggregate with a size of about 0-5 mm for concrete structures, and reuse of demolished concrete lumps (DCLs) with a size much larger than that of recycled aggregate, e.g., 50-300 mm, has been limited to roadbed, backfilling materials, or discarded to landfills. Treatment processes of DCLs are much simpler than those of recycled aggregate, leading to less cost and more energy-saving. In the future, the amount of demolished concrete is estimated to be much higher, so reuse of DCLs for concrete structures will become necessary. The objectives of this paper are to document the process of making reinforced concrete beams with DCLs, and to discuss the flexural and shear behaviors of those reinforced DCL beams through an experimental program, which includes three beams filled with DCLs and one conventional beam for investigating the flexural strengths and deformations, and 12 beams filled with DCLs and two conventional beams for investigating the shear strengths and deformations. The authors hope that the proposed concept offers another sustainable solution to the concrete industry.

Keywords: demolished concrete; reinforced concrete; beams; sustainability; flexural behavior; shear strength

1. Introduction

Concrete has grown to be an essential material for modern society. However, the amount of concrete in use and in stock compared with other materials brings up the issue of the enormous amount of waste generated when concrete is disposed of. As a major user of concrete, the construction industry has addressed this problem and carried out research and development regarding the recycling of concrete since the 1970s (Buck 1977, Frondistou-Yannas 1977). Since

*Corresponding author, Professor, E-mail: bowu@scut.edu.cn
[a]Engineer
[b]Associate Professor
[c]Senior Engineer

then, it has been widely accepted that recycling of construction and demolition wastes for reuse as coarse aggregate in new concrete production offers a sustainable, environmentally responsible and economically viable route to convert this material into a valuable resource (Dhir *et al*. 1999). More recently, Limbachiya *et al*. (2007) showed that commercially produced recycled coarse aggregate (RCA) has chemical and mineralogical characteristics suitable for use in new concrete production. They found that up to 30% RCA, when used as direct replacement of natural gravel, has no influence on the main three oxides (SiO_2, Al_2O_3, and CaO) of concrete if adequate quality control criteria during RCA production are being adopted. Ajdukiewicz and Kliszczewicz (2002) investigated the potential use of aggregates obtained from the crushing of structures with strengths of 40-70 MPa higher quality with large amount of cement. The aggregate obtained from the crushing of structures retained some binding abilities as may be activated by means of silica fume or fly ash admixtures, particularly when the carbonated zone is not too deep.

However, the fine fraction of these recycled aggregates has not been the subject of thorough studies since it is believed that their greater water absorption can jeopardize the final results. An experimental program was conducted by Evangelista and Brito (2007) to study the use of recycled fine aggregates as partial or global replacements of natural fine aggregates in the production of structural concrete. They found that the compressive strength did not seem to be affected by the fine aggregate replacement ratio when up to 30% replacement ratios were used.

Generally, structural members made of recycled aggregate concrete exhibit lower flexural and shear strength compared to similar conventional concrete members (Han *et al*. 2001, Etxeberria *et al*. 2007). But test results of four recycled concrete beams with 50% of recycled coarse aggregates (screened into two size fractions, 4-12 mm and 10-25 mm) and four conventional concrete beams showed that whereas the beams' deflections and ultimate loads were little affected by the different types of concretes (Gonzalez-Fonteboa and Martinez-Abella 2007). Test results of large size beams also indicated that recycled concrete members showed equal or superior flexural and shear performance when compared with the companion conventional concrete members when the recycled aggregate concrete was designed by the EMV (i.e., equivalent mortar volume) method (Fathifazl *et al*. 2009a, b, 2010).

Recycling of demolished concrete could not only help to conserve the depleted natural resources of gravel and sand, but could also help to solve the growing waste disposal problem. In the past decades, however, recycling use of demolished concrete was almost limited to the types of recycled coarse and fine aggregates for concrete structures, and reuse of demolished concrete lumps (DCLs) has been limited to roadbed, backfilling materials, or discarded to landfills. Since treatment processes of DCLs are much simpler than those of recycled aggregates, leading to less cost and more energy-saving, Wu *et al*. (2009) proposed to use DCLs for potential direct applications in concrete structures.

It should be noted that DCL is quite different from recycled aggregate. First, recycled coarse and fine aggregates are generally with a size of about 5-40 mm and a size of about 0-5 mm, respectively, but the size of DCL is much larger than that of recycled aggregate, e.g., 50-300 mm. Secondly, recycled coarse aggregate is generally natural coarse aggregate with a small amount of old mortar (Eguchi *et al*. 2007), but DCL is actually a large amount of old concrete. Thirdly, recycled aggregate has to be mixed with cement, water, and sometimes other necessary materials (e.g., additives, natural aggregate, etc) to produce recycled aggregate concrete, but DCL can be used as old concrete and directly mixed with new concrete made with natural aggregate to form new concrete-old concrete combined structural members, as did in the tests reported in this paper.

The objectives of this paper are to document the process of making reinforced concrete (RC) beams with DCLs, and to discuss the flexural and shear behaviors of those reinforced DCL beams through an experimental program. The authors hope that the proposed concept offers another sustainable solution to the concrete industry.

2. Materials and specimens production

Three RC beams filled with DCLs and one conventional RC beam were tested to reveal the flexural behavior of the beam specimens. The geometries and reinforcement scheme are showed in

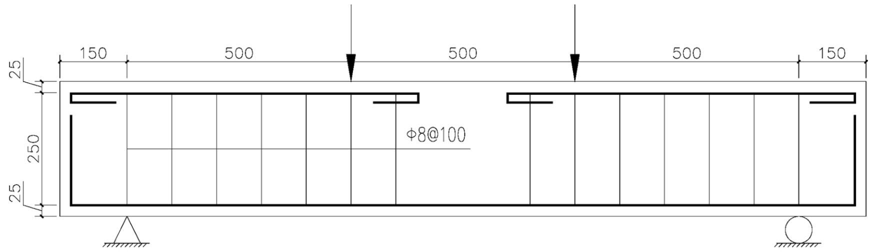

Fig. 1 Schematic diagram of specimens in flexural behavior test (unit: mm; 1 mm = 0.0394 in)

Table 1 Parameters of specimens

Specimen		Sectional width (mm)	Effective depth (mm)	Length (mm)	Clear span (mm)	Diameter of main bar (mm)	Reinforcement ratio	η	λ
Group I for flexural behavior test	RB10	146	270			10	0.4%	20%	-
	B14	146	268	1800	1500	14	0.8%	0	-
	RB14	154	268			14	0.7%	20%	-
	RB18	150	266			18	1.3%	20%	-
Group II for shear behavior test	RB-1	149	262.5				2.5%	20%	1
	RB-1.5	147	262.5				2.5%	20%	1.5
	B-2	146	262.5	1800	1500		2.6%	0	2
	RB-2	148	262.5				2.5%	20%	2
	RB-2-150	154	262.5				2.4%	20%	2
	RB-2-100	149	262.5				2.5%	20%	2
	RB-2.5	144	262.5			25	2.6%	20%	2.5
	B-3-150	152	262.5				2.5%	0	3
	RB-3	147	262.5	2300	2000		2.5%	20%	3
	RB-3-150	156	262.5				2.4%	20%	3
	RB-3-100	145	262.5				2.6%	20%	3
	RB-4	150	262.5				2.5%	20%	4
	RB-4-150	147	262.5	2900	2600		2.5%	20%	4
	RB-4-100	150	262.5				2.5%	20%	4

1 mm = 0.0394 in

Table 2 Strengths of concrete

Specimen	f_{c1u} (MPa)	f_{c2u} (MPa)	f_{cu} (MPa)	f_c (MPa)	f_t (MPa)	f_c' (MPa)
RB10	45.2	32.9	42.7	28.6	2.74	34.2
B14	44.7	-	44.7	29.9	2.81	35.8
RB14	44.7	32.9	42.3	28.3	2.73	33.9
RB18	45.2	32.9	42.7	28.6	2.74	34.2
RB-1	48.8	32.9	45.6	30.5	2.84	36.5
RB-1.5	48.8	32.9	45.6	30.5	2.84	36.5
B-2	49.0	-	49.0	32.8	2.96	39.2
RB-2	49.0	32.9	45.8	30.6	2.85	36.6
RB-2-150	47.0	32.9	44.2	29.6	2.79	35.3
RB-2-100	47.0	32.9	44.2	29.6	2.79	35.3
RB-2.5	53.4	32.9	49.3	33.0	2.97	39.4
B-3-150	47.1	-	47.1	31.5	2.89	37.7
RB-3	53.4	32.9	49.3	33.0	2.97	39.4
RB-3-150	47.1	32.9	44.3	29.6	2.80	35.4
RB-3-100	50.4	32.9	46.9	31.4	2.89	37.5
RB-4	51.5	32.9	47.8	32.0	2.92	38.2
RB-4-150	53.0	32.9	49.0	32.8	2.96	39.2
RB-4-100	53.0	32.9	49.0	32.8	2.96	39.2

1 MPa = 145 psi

Note: f_{c1u}, f_{c2u} - cubic compressive strengths of the cast-in-situ concrete and demolished concrete on the testing day, respectively; $f_{cu} = [f_{c1u} \cdot (1-\eta) + f_{c2u} \cdot \eta]$ - combined cubic compressive strength of the cast-in-situ concrete and demolished concrete; $f_c = 0.88 \times 0.76 f_{cu}$ - combined prismatic compressive strength of the cast-in-situ concrete and demolished concrete; $f_t = 0.88 \times 0.395 f_{cu}^{0.55}$ combined tensile strength of the cast-in-situ concrete and demolished concrete; $f_c' = 0.8 \times f_{cu}$ combined cylinder compressive strength of the cast-in-situ concrete and demolished concrete.

Fig. 1. The cross section of the specimen is 150 mm (5.91 in.) in width and 300 mm (11.81 in.) in depth. Steel bars of HRB335, which are crescent ribbed bars with diameters of 10, 14 and 18 mm (0.39, 0.55 and 0.71 in.) and measured yield strengths of 356, 363 and 384 MPa (51.63, 52.65 and 55.69 ksi), were, respectively, used as longitudinal rebars in this investigation. The clear concrete cover to the longitudinal bars is 25 mm (0.98 in.). Tables 1 and 2 show the details of the four specimens. In the specimen label, for example, "RB" means RC beams filled with DCLs, and "B" means conventional RC beams. In Table 1, "η" means the mix ratio (i.e., a ratio of the mass of DCLs to the total concrete mass of the specimen), and "λ" means the shear span ratio (i.e., the ratio of shear span to effective depth of the section).

Also shown in Tables 1 and 2 are twelve RC beams filled with DCLs and two conventional RC beams. These 14 beams were tested to reveal the shear behavior of the specimens. Seven of the 14 beams have stirrups while the other specimens are beams without stirrups. Steel bars of HPB235 with a diameter of 6.5 mm (0.26 in.) are used as stirrups in the beams. The longitudinal reinforcing bars of the 14 beams are HRB335 steel bars with a diameter of 25 mm (0.98 in.). The yield strengths of the stirrup and longitudinal reinforcing bars are 346 and 414.4 MPa (50.18 and 60.10

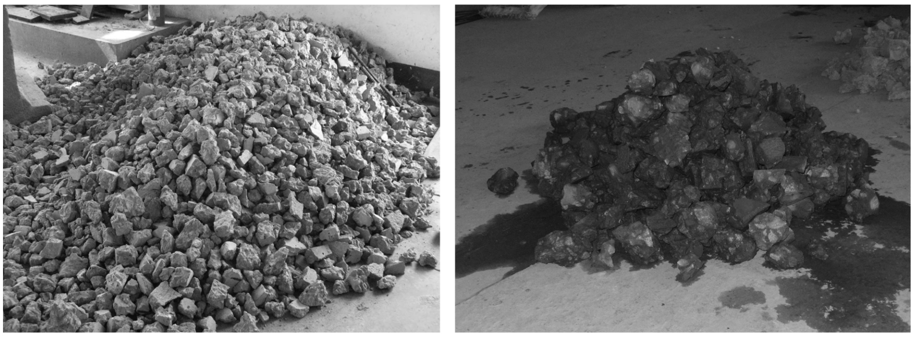

(a) (b)

Fig. 2 Demolished concrete lumps

Table 3 Concrete mix proportion

Cast-in-situ concrete				Demolished concrete			
Water (kg/m^3)	Cement (kg/m^3)	Sand (kg/m^3)	Coarse aggregate (kg/m^3)	Water (kg/m^3)	Cement (kg/m^3)	Sand (kg/m^3)	Coarse aggregate (kg/m^3)
202	460	640	1200	175	343	621	1261

1 kg = 2.2046 lb; 1 m^3 = 35.3147 ft^3

Note: Demolished concrete is the original concrete from which the demolished concrete lumps (DCLs) were obtained. The demolished concrete is old concrete and was made with natural aggregates (not recycled aggregates).

ksi), respectively. The clear concrete cover to the longitudinal bars is 25 mm (0.98 in.).

The cast-in-situ concrete was made of Portland blast furnace-slag cement (P.S.A32.5), natural limestone crushed rock coarse aggregates with two size fractions (5-10 mm, i.e., 0.197-0.394 in. and 10-20 mm, i.e., 0.394-0.787 in.), and river sands (0-4 mm, i.e., 0-0.157 in) from a local source. Table 3 shows the concrete mix proportions of the cast-in-situ concrete and demolished concrete. The demolished concrete was from the residual concrete beams used in a previous testing program one year ago. The old residual beams were conserved in the laboratory. They were from 1200 mm (47.24 in.) to 2000 mm (78.74 in.) long, and had a rectangular cross section of 100 mm (3.94 in.) by 200 mm (7.87 in.). The cement, and natural coarse and fine aggregates used for the old residual beams were the same as those for the cast-in-situ concrete. These old beams were broken up manually. The size of the lumps is about 50 mm (1.97 in.) to 100 mm (3.94 in.), as shown in Fig. 2.

Fabricated steel cages were fixed in the wooden moulds, which were made according to the predetermined dimensions. Firstly, cast a layer of cast-in-situ concrete about 30 mm (3.94 in.) thick, and then put the demolished concrete lumps and cast-in-situ concrete in the mould alternately, finally vibrate the concrete till compacting. Fig. 3 shows a part of the beam under casting. When casting beams, 150 × 150 × 150 mm (5.91 × 5.91 × 5.91 in.) cubes were prepared in steel moulds, and then cured in the same situation as the beams for 28 days. These cubes were used to obtain the cubic compressive strength of the cast-in-situ concrete. The cubic compressive strength of the demolished concrete on the testing day was obtained by the residual cubes made when the old beams were cast.

Fig. 3 Beams under casting

3. Flexural behavior

As shown in Fig. 4, all the four beams for flexural behavior tests were tested under two-point loading. Each specimen was preloaded before the actual loading in order to adjust the loading system and the measuring device. In the actual loading, each loading stage was about 10 percent of the predicted ultimate load. At three minutes later, data was collected. The magnitude of the load increment was reduced when approaching the predicted cracking load and the ultimate load.

A load cell was used to record the load in the loading process. Dial indicators with a range of 50 mm (1.97 in.), which were placed over the supports and under the midpoint of the beam, were

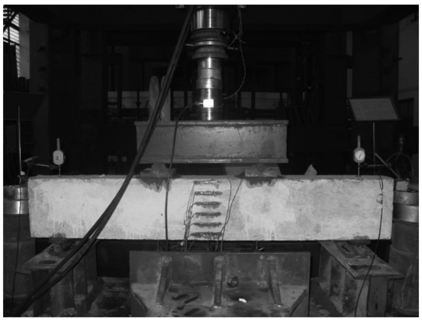

Fig. 4 Loading apparatus

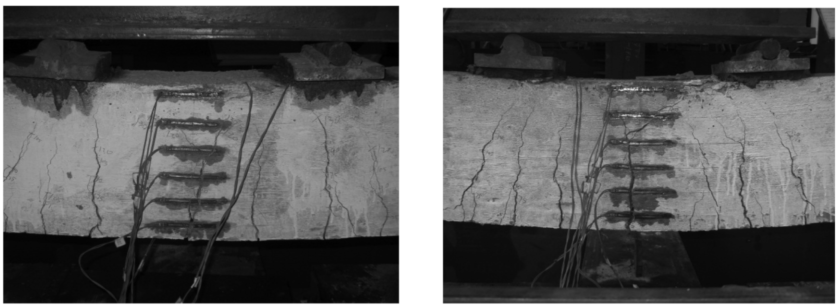

(a) B14 (b) RB14

Fig. 5 Failure modes of two specimens in flexural behavior test used to measure the vertical deformation. Strains of longitudinal bars were measured by the stain gauges located at the mid-span of the beam, and were attached to the longitudinal bars and embedded in concrete in advance. Strains of concrete in the mid-span of the beam were measured by the strain gauges, which were attached to the surface of beam side (see Figs. 4 and 5).

4.1 General observation and failure patterns

At the beginning of the loading, each specimen was in the elastic stage. Strains of the longitudinal bars and the concrete at the same height were approximately equal to each other and small. As the load was increased, concrete at the edge of the tensile zone in the mid-span of the beam cracked as the strain of the longitudinal bars suddenly increased. As the load was continuously increased, new cracks appeared in succession and extended upward, while the depth of compression region decreased. The deflection of the mid-span increased faster than that in the elastic stage. All of the four specimens presented the same failure patterns as the proper RC beams. Generally speaking, the failure mode of the RC beams filled with DCLs was similar to that of the conventional RC beam. Fig. 5 shows the failure modes of two specimens.

4.2 Load-deflection curves

Fig. 6 shows the measured load-deflection curves. It shows that: (a) the load-deflection trend of the RC beams filled with DCLs is similar to that of the conventional RC beam; (b) the initial stiffnesses of the specimens “RB14” and “B14” are almost the same; and (c) the load-deflection curves of the specimens “RB14” and “B14” are almost coincident, which shows that the flexural behavior of RC beam filled with DCLs is similar to that of conventional RC beam in the same condition.

4.3 Flexural capacity and cracking moment

Test results of all the four specimens are listed in Table 4. Please note that the yielding load corresponds to the load when the longitudinal reinforcements yielded, and the ultimate load corresponds to the load when the specimen ultimately failed.

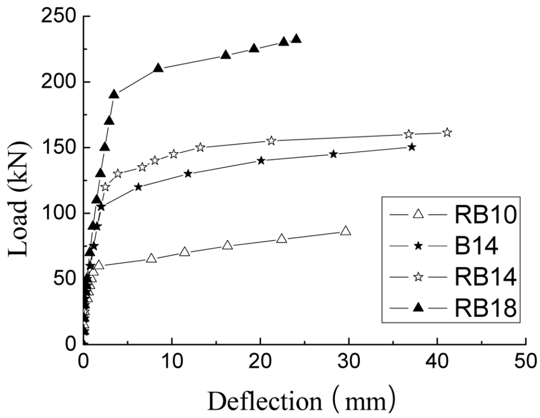

Fig. 6 Load-deflection curves in flexural behavior test (1 mm = 0.0394 in; 1 kN = 0.225 lbf)

Table 4 Test results of specimens in Group I

Specimen	Cracking load (kN)	Cracking moment at mid-span (kN m)	Yielding load (kN)	Yielding moment at mid-span (kN m)	Ultimate load (kN)	Flexural capacity at mid-span (kN m)
RB10	32.5	8.13	58	14.5	85.9	21.5
B14	42.5	10.63	98	24.5	150.4	37.6
RB14	37.5	9.38	107	26.8	161.4	40.4
RB18	35.0	8.75	190	47.5	232.1	58.0

1 kN = 0.225 lbf; 1 kN m = 0.738 ft-kips

Table 5 Comparison of calculation results with test results for flexural capacity

Specimen	Measured (kN m)	GB50010-2002		ACI318-08	
		Calculated (kN m)	(Calculated - Measured) / Measured	Calculated (kN m)	(Calculated - Measured) / Measured
RB10	21.5	14.7	-31%	14.7	-31%
B14	37.6	28.5	-24%	28.6	-24%
RB14	40.4	28.5	-29%	28.6	-29%
RB18	58.0	47.6	-18%	47.7	-18%

1 kN m = 0.738 ft-kips
Note: f_c and f_c' listed in Table 2 are, respectively, used in the formulas in GB50010-2002 and ACI318-08.

Table 6 Comparison of calculation results with test results for cracking moment

Specimen	Measured (kN m)	GB50010-2002				ACI318-08			
		Calculated (kN m)	(Calculated - Measured) / Measured	Modified (kN m)	(Modified - Measured) / Measured	Calculated (kN m)	(Calculated - Measured) / Measured	Modified (kN m)	(Modified - Measured) / Measured
RB10	8.13	9.85	21%	7.88	-3%	8.43	4%	8.01	-1%
B14	10.63	10.59	-0.4%	-	-	9.02	-15%	-	-
RB14	9.38	10.80	15%	8.64	-8%	9.24	-1%	8.78	-6%
RB18	8.75	11.21	28%	8.97	3%	9.58	10%	9.10	4%

1 kN m = 0.738 ft-kips
Note: 1) f_t and f_c' listed in Table 2 are, respectively, used in the formulas in GB50010-2002 and ACI318-08;
2) Modified cracking moment = 0.8 × Calculated cracking moment using GB50010-2002, and Modified cracking moment = 0.95 × Calculated cracking moment using ACI318-08.

Table 5 shows the comparison between flexural capacities calculated according to the formulas in GB50010-2002 and ACI318-08 and the testing data. It shows that: (a) flexural capacities of RC beams filled with DCLs calculated by the formulas in GB50010-2002 and ACI318-08 are both on average 26% lower than the test results, while flexural capacities of the conventional RC beam ("B14") calculated by the formulas in GB50010-2002 and ACI318-08 are both 24% lower than the test result, indicating that the flexural capacities calculated using formulas in GB50010-2002 and ACI318-08 have a similar safety margin for conventional RC beams and RC beams filled with DCLs; and (b) the flexural capacity of “RB14” is close to that of “B14”.

Table 6 shows the comparison between cracking moments calculated according to the formulas in GB50010-2002 and ACI318-08 and the testing data. It shows that: (a) The cracking moments of RC beams filled with DCLs can not be estimated safely by formulas in GB50010-2002 and ACI318-08 which are proposed for conventional RC beams, and it is necessary to modify the codes. To solve this problem, we suggest that adjusting factors of 0.8 (for GB50010-2002) and 0.95 (for ACI318-08) be, respectively, adopted for the initial calculated cracking moments of RC beams filled with DCLs. It can be seen that the modified cracking moments based on the formulas in GB50010-2002 on average are 2.67% lower than the test results, while the modified cracking moments based on the formulas in ACI318-08 are on average 1% lower than the test results. (b) In the same condition, the measured cracking moment of “RB14” is 12% lower than that of “B14”. This is because that the interfaces between the new and old concrete in a RC beam filled with DCLs may become the weak region when the beam is subjected to tension, which makes the vertical crack easier to appear and develop.

5. Shear behavior

The test setup and instrumentation are similar to the flexural tests as discussed earlier, but the distances between the supports and the loading points are not constant for the fourteen specimens to achieve different shear span ratio “λ” in Table 1. Strains of longitudinal bars and transverse stirrups were measured by the stain gauges, which were attached to the longitudinal bars/transverse stirrups and embedded in concrete in advance.


(a) RB-1

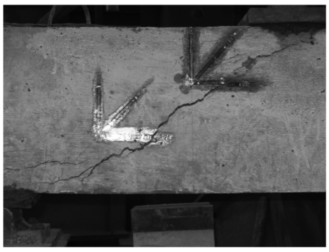
(b) RB-2


(c) RB-3-150


(d) RB-3


(e) RB-4


(f) RB-4-100

Fig. 7 Failure modes of some specimens in shear behavior test

5.1 General observation

Most beams showed shear failure modes during the test: inclined compression, shear compression and diagonal tension according to different shear span ratios. Three of the fourteen beams showed bending failure due to the large shear span ratio. Fig. 7 shows the failure modes of some of these specimens.

5.1.1 Inclined compression failure

Specimen presented inclined compression failure while the shear span ratio is small (λ = 1). Take Beam "RB-1" without stirrups for example. A diagonal crack of 110 mm (4.33 in.) long at 60^o appeared in the shear span on the same side as the loading point when the concentric load was 160 kN (35.97 kips). When loading up to 180 kN (40.46 kips), a diagonal crack of 70 mm (2.76 in.) long and 0.05 mm (0.002 in.) wide at 45^o direction started to appear in the middle of the shear span. After the load was increased to 440 kN (98.91 kips), two diagonal cracks with the maximum width of about 0.6 mm (0.024 in.), generally paralleling each other, were found in the shear span. Finally, concrete between the loading and the supporting points was crashed under diagonal compressive stress with the loading up to 481.4 kN (108.22 kips). The failure mode was similar to that of oblique stub column under axial compression.

5.1.2 Shear compression failure

Shear compression failure happened to the following beams (a) "RB-1.5", "B-2", "RB-2" and "RB- 2.5" without stirrups and have a shear span ratio of 1.5 ≤ λ ≤ 2.5; (b) "RB-2-150" and "RB-2-100" with stirrups and have a shear span ratio of λ = 2; (c) "B-3-150" and "RB-3-150" with stirrups and have a shear span ratio of λ = 3 but spacing of stirrup legs was relatively larger. With the increase of the load, diagonal cracks occurred in the web. The longest and widest crack became the critical diagonal crack. With the continued increase of the load, diagonal cracks were widened. Finally, the concrete of the shear compression zone, located on the upside of the diagonal crack under the loading point was decreased into a small area, crushed under the combined shear stress and compressive stress.

5.1.3 Diagonal tension failure

Beams "RB-3" and "RB-4" without stirrups and a large shear span ratio (λ ≥ 3) displayed a diagonal tension failure. Take specimen "RB-3" for an example. The flexural cracks appeared at the bottom of the mid-span. Then, diagonal cracks started to form in the shear span. When the load was increased to 110 kN (24.73 kips), the diagonal crack in the middle of the shear span was about 300 mm (11.81 in.) in length and 0.1 mm (0.004 in.) in width along the direction from the loading point to the support point. After that, the diagonal crack quickly grew in length and in width. Finally, the diagonal tension failure happened to the specimen when the load was increased to 131.2 kN (29.49 kips). Compared with specimen "RB-3", failure of specimen "RB-4" happened more abruptly.

5.1.4 Flexural failure

Beams with stirrups displayed a typical flexural failure when the shear span ratio was λ = 3 and the spacing of the stirrup legs was relatively small such as specimen "RB-3-100" or the shear span ratio λ = 4 such as specimens "RB-4-150" and "RB-4-100". The final failure behavior was displayed as the crushing of concrete of the compression zone.

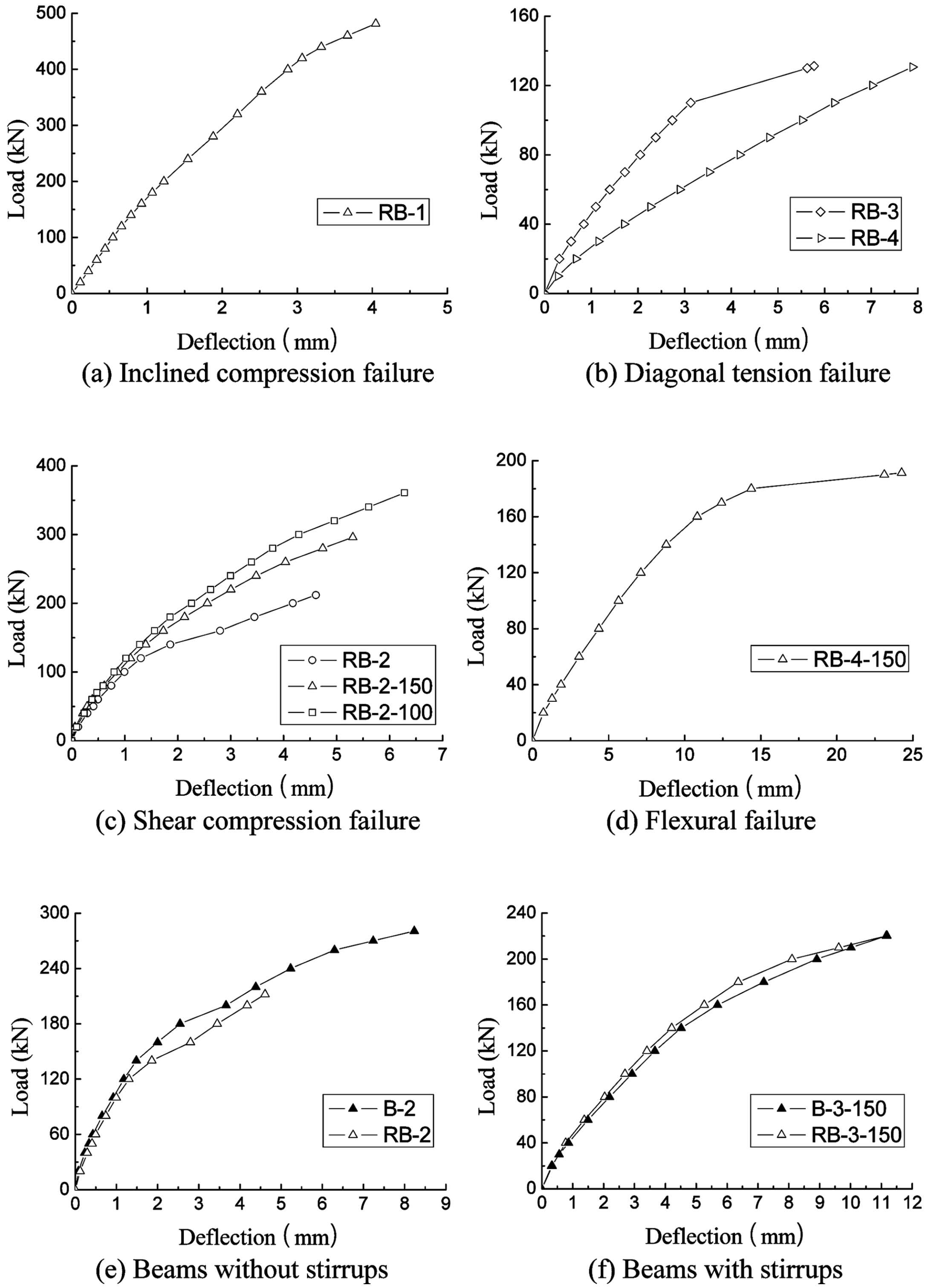

Fig. 8 Load-deflection curves in shear behavior test (1 mm = 0.0394 in; 1 kN = 0.225 lbf)

5.2 Load-deflection curves

Fig. 8 shows the load-deflection curves of some of the specimens. From Fig. 8, it can be seen that: (a) For beams without stirrups in which either the inclined compression failure or the diagonal tension failure happened, load-deflection curves evidently displayed a linear character before achieving 80% of the failure load, and the slope of the curves decreased after that. The slope at the end of the curve for specimen “RB-3” is relatively flatter because of the expansion of the critical diagonal crack, while specimen “RB-4” does not show the flat end because its critical diagonal crack showed up suddenly and had no warning as the failure happened quickly. (b) For beams with and without stirrups in which the shear compression failure occurred, the slope of the load-deflection curve is decreased gradually with the increase of the loading, while the nonlinear character with a gradual change evidently displayed at the same time. (c) For beams with stirrups in which flexural failure occurred, the load-deflection curves increase linearly at the beginning. The slope is decreased gradually at the upper stage and the curves almost go horizontal when the final

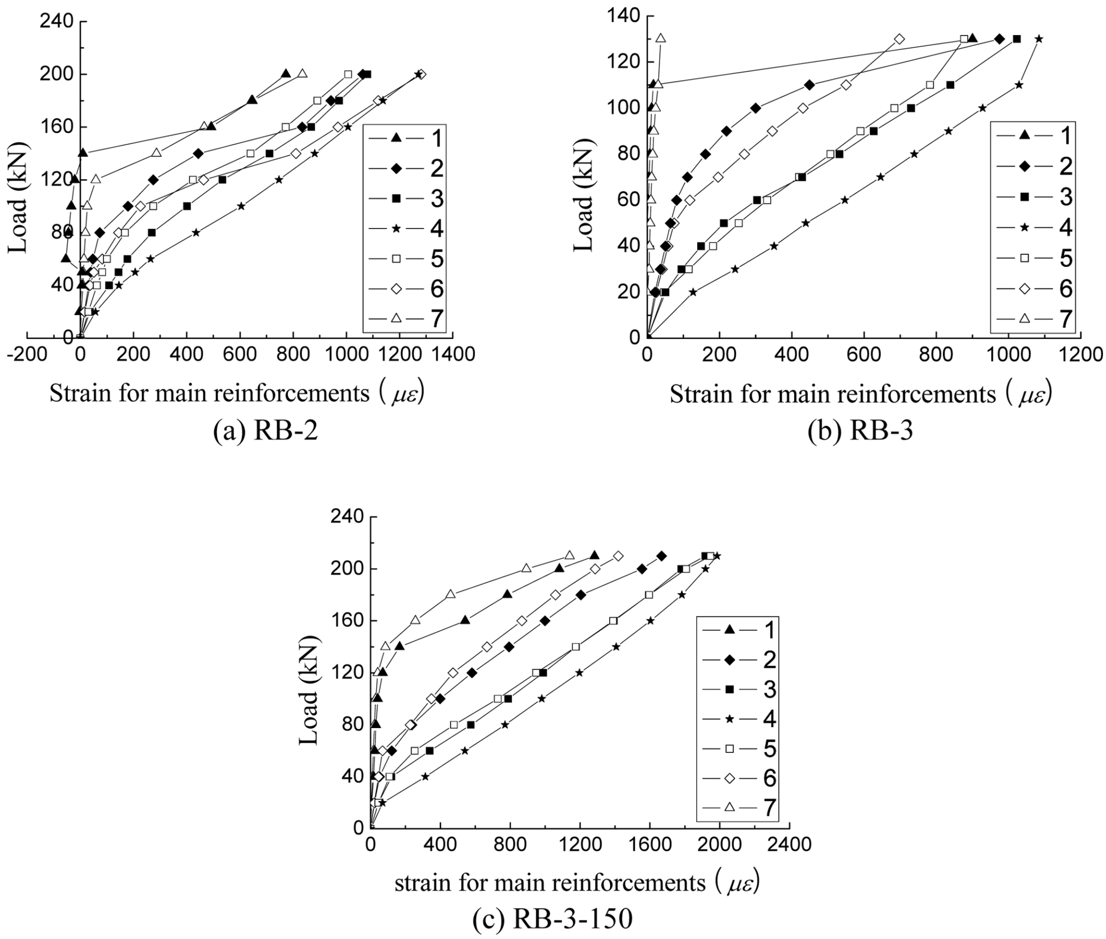

Fig. 9 Load-strain curves for main reinforcements (1 kN = 0.225 lbf)

failure happened. The corresponding deflection at the mid-span is larger than those in the beams which showed the inclined compression failure, the diagonal tension failure and the shear compression failure. (d) With or without stirrups, the load-deflection curves of RC beams filled with DCLs are close to that of the conventional RC beam in the same condition. Both types of beams had almost the same initial stiffness. However, the failure load of the former one was lower than that of the latter one especially for beams without stirrups.

5.3 Load-strain curves for main reinforcements

Test results show that the main reinforcements in beams without stirrups and beams with stirrups with a shear span ratio λ = 2 did not yield when the beams were crushed. However, the main reinforcements in the beams with stirrups with a shear span ratio of $\lambda \geq 3$ yielded. Fig. 9 shows the load-strain curves for main reinforcements of some specimens. The corresponding locations of strain gauges at main reinforcements are shown in Fig. 10. From Figs. 9 and 10, the maximum strain of the main reinforcement occurred in the mid-span at the beginning of the loading process because of the maximum moment there. With the increasing of the loading, the strain of the main reinforcements grew at any place along the span, but it grew faster around the support area than in the mid-span at the upper loading process.

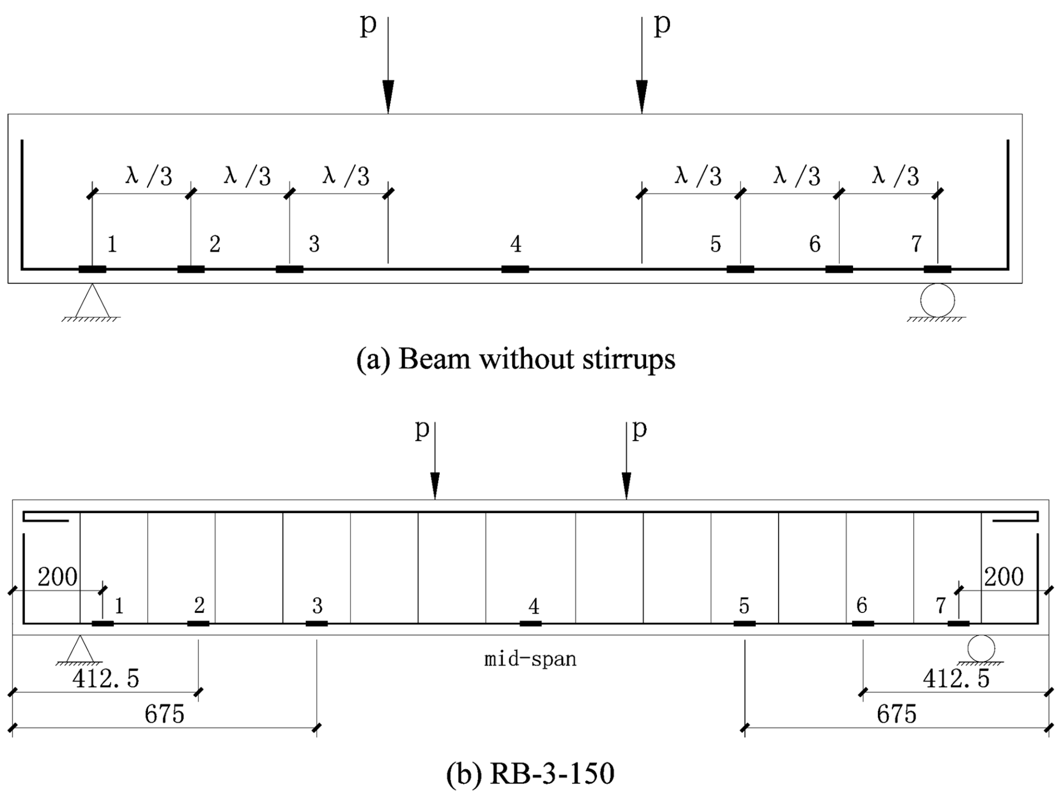

Fig. 10 Locations of strain gauges at main reinforcements for some specimens (unit: mm; 1 mm = 0.0394 in)

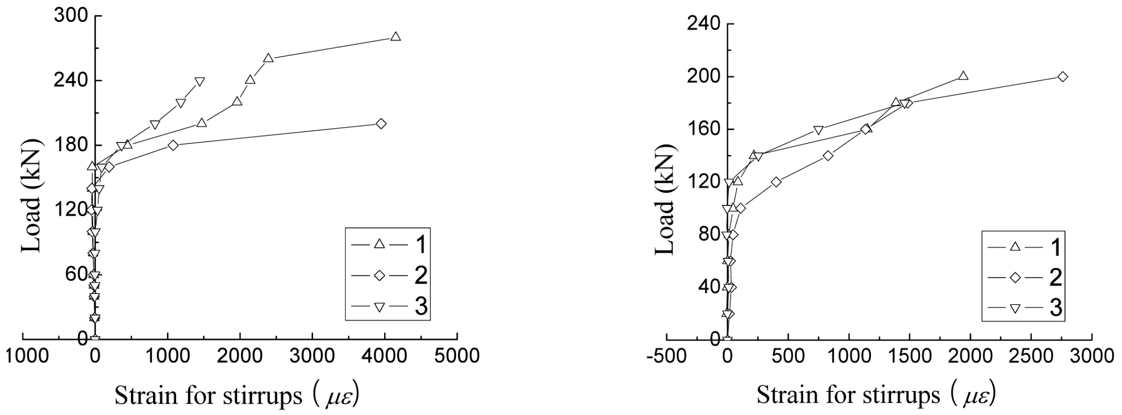

(a) RB-2-150 (b) RB-3-150

Fig. 11 Load-strain curves for stirrups (1 kN = 0.225 lbf)

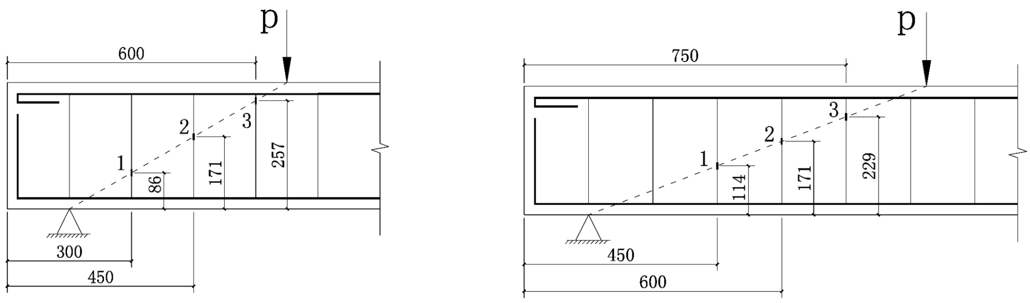

(a) RB-2-150 (b) RB-3-150

Fig. 12 Locations of strain gauges at stirrups for some specimens (unit: mm; 1 mm = 0.0394 in)

5.4 Load-strain curves for stirrups

Fig. 11 shows the load-strain curves of stirrups in some specimens, and Fig. 12 shows the locations of strain gauges at stirrups. From Figs. 11 and 12, it can be seen that for the RC beams filled with DCLs with stirrups, the strain of stirrups was lower before diagonal cracking occurred. The same was true for conventional RC beams. It can also be seen that with the increase of the load, the strain of stirrups across the diagonal cracks has obviously increased.

5.5 Shear strength

Test results of the specimens are listed in Table 7. In Table 7, the cracking load corresponds to the beam's first diagonal cracking load, the ultimate load was determined based on GB50152-92, and the shear strength is regarded as half the ultimate load.

A comparison of specimens "RB-2" and "B-2" in Table 7 shows that the cracking load, shear strength and failure load of the RC beam filled with DCLs without stirrups are 25%, 14.3% and

Table 7 Test results of specimens in Group II

Specimen	Cracking load for first diagonal crack (kN)	Ultimate load (kN)	Failure load (kN)	Shear strength (kN)	Failure mode
RB-1	150	481.4	481.4	240.7	Inclined Compression
RB-1.5	130	320	341.6	160	Shear Compression
B-2	120	210	280.6	105	Shear Compression
RB-2	90	180	212	90	Shears Compression
RB-2-150	90	270	296.1	135	Shear Compression
RB-2-100	120	350	360.9	175	Shear Compression
RB-2.5	75	150	195.1	75	Shear Compression
B-3-150	70	190	220.3	95	Shear Compression
RB-3	85	120	131.2	60	Diagonal Tension
RB-3-150	70	190	218.8	95	Shear Compression
RB-3-100	90	-	240.6	-	Bending
RB-4	55	130.6	130.6	65.3	Diagonal Tension
RB-4-150	60	-	191.3	-	Bending
RB-4-100	70	-	190.8	-	Bending

1 kN = 0.225 lbf

24.4% lower than those of the conventional RC beam without stirrups, respectively. This is partly because the combined strength of the demolished concrete and cast-in-situ concrete inside the former one was lower than that of the cast-in-situ concrete in the latter one (see Table 2), and partly because the interfaces between old and new concrete may become a weak area.

A comparison of specimens “RB-3-150” and “B-3-150” in Table 7 shows that the cracking load, shear strength and failure load of the RC beam filled with DCLs with stirrups are almost the same as that of the conventional RC beam with stirrups, which means that the two factors discussed earlier have little influence on beams with stirrups.

Fig. 13 shows the shear strength-shear span ratio curve of RC beams filled with DCLs without stirrups. It can be found that the behavior of RC beams filled with DCLs without stirrups is similar to that of conventional RC beams without stirrups. Shear strength decreased gradually with the increase of the shear span ratio, as discussed by Ma and Tadros (1999). While the shear span ratio is greater than 3.0, shear strength changes little with the change of the shear span ratio.

By the regression analysis of data in Fig. 13, the shear strength calculation formula of the RC beam filled with DCLs without stirrups under the concentrated load with the shear span ratio from 1.0 to 4.0 can be determined as follow

$$V_u = \frac{1.4}{\lambda - 0.29} f_t b h_0 \quad (\lambda \le 3) \tag{1}$$

in which V_u is the shear strength; λ is the shear span ratio; b and h_0 are, respectively, the sectional width and effective depth of the beam; and f_t is the combined tensile strength of the cast-in-situ concrete and demolished concrete.

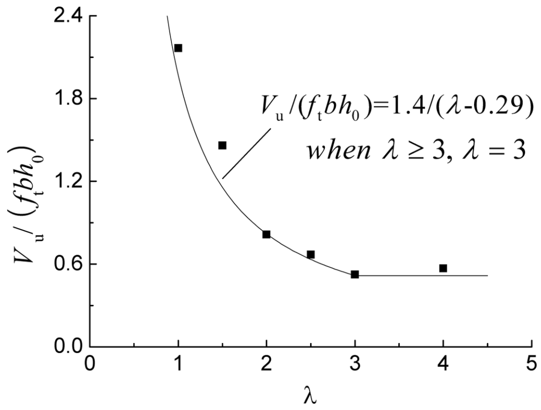

Fig. 13 Shear strength - shear span ratio curve (V_u is the shear strength; b and h_0 are, respectively, the sectional width and effective depth of beam; f_t is the combined tensile strength of cast-in-situ concrete and demolished concrete)

Table 8 Comparison of calculation results with test results for shear strength

Specimen	V_u (kN)	V_1 (kN)	$\frac{V_1 - V_u}{V_u}$	V_2 (kN)	$\frac{V_2 - V_u}{V_u}$	V_3 (kN)	$\frac{V_3 - V_u}{V_u}$
RB-1	240.7	77.8	-68%	40.2	-83%	219.1	-9%
RB-1.5	160	76.8	-52%	39.6	-75%	126.8	-21%
B-2	105	66.1	-37%	40.8	-61%	92.8	-12%
RB-2	90	64.5	-28%	40.0	-56%	90.6	1%
RB-2-150	135	105.8	-22%	80.8	-40%	132.4	-2%
RB-2-100	175	123.7	-29%	99.5	-43%	149.4	-15%
RB-2.5	75	56.1	-25%	40.4	-46%	71.0	-5%
B-3-150	95	90.5	-5%	81.6	-14%	99.5	5%
RB-3	60	50.1	-17%	41.2	-31%	59.1	-1%
RB-3-150	95	90.0	-5%	81.4	-14%	99.1	4%
RB-3-100	-	108.0	-	99.6	-	116.7	-
RB-4	65.3	50.2	-23%	41.4	-37%	59.3	-9%
RB-4-150	-	89.9	-	81.0	-	98.9	-
RB-4-100	-	110.9	-	101.8	-	120.1	-

1 kN = 0.225 lbf

Note: V_u is the measured shear strength; V_1 and V_2 are the calculated shear strengths according to GB50010-2002 and ACI318-2008, respectively; and V_3 is the calculated shear strength using Eqs. (1) and (2). f_t listed in Table 2 is used in the calculations.

Shear strength of RC beams filled with DCLs with stirrups can be obtained by adding the contribution of stirrup into Eq. (1). The shear strength of RC beams filled with DCLs with stirrups under the concentrated load can then be calculated as follow

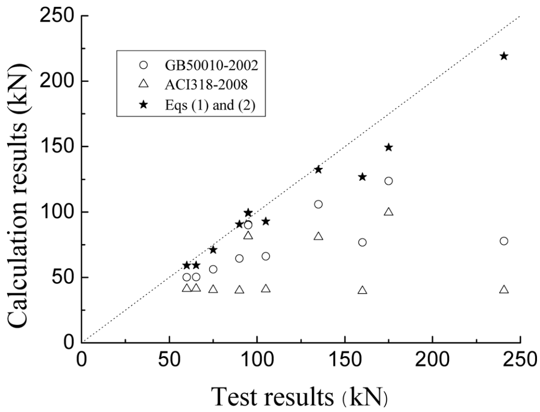

Fig. 14 Comparison of calculation results with test results for shear strength (1 kN = 0.225 lbf)

$$V_u = \frac{1.4}{\lambda - 0.29} f_t b h_0 + f_{yv} \frac{A_{sv}}{s} h_0 \quad (\lambda \le 3) \tag{2}$$

in which f_{yv} is the yield strength of stirrups; A_{sv} is the total cross-section area of stirrups; and s is the spacing of stirrup legs.

Table 8 and Fig. 14 show the comparison between the measured shear strength and the data calculated according to Eqs.(1) and (2) and that based on the formulas in GB50010-2002 and ACI318-08. The following conclusions can be made:

(a) The shear strengths of RC beams filled with DCLs without stirrups calculated by formulas in GB50010-2002 and ACI318-08 are 17%~68% and 31%~83% lower than the test results, respectively. This is because formulas given in GB50010-2002 and ACI318-08 are generally conservative.

(b) The shear strengths of RC beams filled with DCLs with stirrups calculated by formulas in GB50010-2002 and ACI318-2008 are 5%~29% and 14%~43% lower than the test results, respectively. However, by comparing Specimen "RB-3-150" and Specimen "B-3-150", similar safety factors can be achieved when using those code articles.

(c) The shear strengths of RC beams filled with DCLs without stirrups calculated using Eq. (1) meet well with the test results.

(d) The shear strengths of RC beams filled with DCLs with stirrups calculated using Eq. (2) agree well with the test results.

6. Conclusions

The flexural behavior and shear behavior of RC beams filled with DCLs were investigated through an experimental program. The effectiveness of formulas in GB50010-2002 and ACI318-08 for the cracking moment and flexural capacity of RC beam filled with DCLs is discussed. A formula is proposed for the shear strength of RC beam filled with DCLs based on the test data. Test results show the following:

(a) The flexural behavior of RC beams filled with DCLs is generally similar to that of conventional RC beams in the same condition. The flexural capacities calculated using formulas in GB50010-2002 and ACI318-08 have a similar safety margin for conventional RC beams and RC beams filled with DCLs, but the cracking moments of RC beams filled with DCLs can not be estimated safely by formulas in GB50010-2002 and ACI318-08, and adjusting factors of 0.8 (for GB50010-2002) and 0.95 (for ACI318-08) may be, respectively, adopted for the initial calculated cracking moments of RC beams filled with DCLs.

(b) For the specimens without stirrups in shear behavior test, the load-deflection curve of the RC beam filled with DCLs is close to that of the conventional RC beam in the same condition, but the failure load of the former one is much lower than that of the latter one. The cracking load, shear strength and failure load of the RC beam filled with DCLs with stirrups are almost the same as those of the conventional RC beam with stirrups.

(c) The shear strengths of RC beams filled with DCLs with stirrups calculated by formulas in GB50010-2002 and ACI318-2008 are 5%~29% and 14%~43% lower than the test results, respectively. However, by comparing Specimen "RB-3-150" and Specimen "B-3-150", similar safety factors can be achieved when using those code articles.

(d) The shear strengths of RC beams filled with DCLs with stirrups calculated using Eq. (2) meet well with the test results.

Acknowledgements

The research reported here was financially supported by the National Natural Science Foundation of China (51025829), Government of Guangdong Province of China (2009B060700094), State Key Laboratory of Subtropical Building Science of China (2008ZB15, 2011ZB07), and South China University of Technology (2009zz0046). Visit to South China University of Technology by the third author was made possible by Department of Civil and Environmental Engineering of University of Tennessee Knoxville.

References

ACI Committee 318 (2008), Building Code Requirements for Structural Concrete (ACI 318-08). Farmington Hills, MI: American Concrete Institute International.

Ajdukiewicz, A. and Kliszczewicz, A. (2002), "Influence of recycled aggregates on mechanical properties of HS/HPC", *Cement Concrete Compos.*, **24**, 269-279.

Buck, A.D. (1977), "Recycled concrete as a source of aggregate", *ACI J.,* **74**, 212-219.

Dhir, R.K., Limbachiya, M.C. and Leelawat, T. (1999), "Suitability of recycled concrete aggregate for use in BS5328 designated mixes", *Proceedings of the Institution of Civil Engineers – Structures and Buildings*, **134**(3), 257-274.

Eguchi, K., Teranishi, K., Nakagome, A. and Kishimoto, H. (2007), "Application of recycled coarse aggregate by mixture to concrete construction", *Constr. Build. Mater.*, **21**(7), 1542-1551.

Etxeberria, M., Mari, A.R. and Vazquez, E. (2007), "Recycled aggregate concrete as structural material", *Mater. Struct*., **40**, 529-541.

Evangelista, L. and Brito, J. (2007), "Mechanical behavior of concrete made with fine recycled concrete aggregates", *Cement Concrete Compos.*, **29**(5), 397-401.

Fathifazl, G., Razaqpur, A.G., Isgor, O.B., Abbas, A., Fournier, B. and Foo, S. (2009a), "Shear strength of steel reinforced recycled concrete beams without stirrups", *Mag. Concr. Res*., **61**(7), 387-400.

Fathifazl, G., Razaqpur, A.G., Isgor, O.B., Abbas, A., Fournier, B. and Foo, S. (2009b), "Flexural performance of steel reinforced recycled concrete (RRC) beams", *ACI Struct. J.*, **106**(6), 858-867.

Fathifazl, G., Razaqpur, A.G., Isgor, O.B., Abbas, A., Fournier, B. and Foo, S. (2010), "Shear strength of steel reinforced recycled concrete beams with stirrups", *Mag. Concr. Res.*, **62**(10), 685-699.

Frondistou-Yannas, S.T. (1977), "Waste concrete as aggregate for new concrete", *ACI J.,* **74**(8), 373-376.

Gonzalez-Fonteboa, B. and Martinez-Abella, F. (2007), "Shear strength of recycled concrete beams", *Constr. Build. Mater.*, **21**, 887-893.

Han, B.C., Yun, H.D. and Chung, S.Y. (2001), "Shear capacity of reinforced concrete beams made with recycled-aggregate", *ACI Special Publications*, **200**, 503-516.

Limbachiya, M.C., Marrocchino, E. and Koulouris, A. (2007), "Chemicalmineralogical characterization of coarse recycled concrete aggregate", *Waste Management*, **27**(2), 201-208.

Ma, Z.J. and Tadros, M.K. (1999), "Simplified method for shear design based on AASHTD load and resistance factor design specifications", Journal of the Transportation Research Board, No.1688, National Research Council, National Academy Press.

National Standard of the People's Republic of China (2002), Code for design of concrete structures (GB50010-2002), Beijing: China Architecture & Building Press. (in Chinese)

National Standard of the People's Republic of China (1992), Testing methods of concrete structure (GB50152-92), Beijing: China Architecture & Building Press. (in Chinese)

Wu, B., Zhao, X.Y., Liu, W., Liu, Q.X. and Xu, Z. (2009), "Test behaviors and numerical analysis of stub steel tubular columns filled with recycled concrete segment/lump and subjected to axial force" *Proceedings of the International Symposium on Innovation & Sustainability of Structures in Civil Engineering*, **1**, 70-76.